

Calculation of cluster decays half-lives for nuclei between $56 < Z_p < 120$ by using temperature dependent proximity model

V. Zanganeh^{1,*}

¹ *Department of Physics, Sciences Faculty,
Golestan University, P. O. Box 49138-15759, Gorgan, Iran*

submitted at : Chinese Physics C

Abstract

Cluster decays half-lives of elements with proton numbers between $56 < Z_p < 120$ are calculated by applying temperature dependent proximity potential approach. For showing the influence of temperature on cluster decays, we compared the results among temperature dependent and independent case with experimental values. The obtained results of the present investigation reveal that we have more accurate results for temperature dependent proximity potential in comparison to ignoring one. In the present work, we find that results provided with temperature dependent proximity model are reasonable estimates for cluster decays half-lives and provide reliable predictions for other super heavies cluster decays.

Key words: Cluster decays, half-lives, temperature dependent, proximity model.

PACS: 23.70.+j

*Electronic address: zanganeh_vahid@yahoo.com ; v.zanganeh@gu.ac.ir

I. INTRODUCTION

Spontaneous cluster decays, heavier than alpha particles but lighter than a fission fragment, of super heavy nuclei is one of most dominant decay chains which happens before spontaneous fission. However, the cluster decays and half-lives of the super heavy nuclei gives us information about the island of stability regions and hence help us to understand the nuclear structure of the daughter as well as parents nuclei[1, 2]. experimentally and theoretically, emitted clusters from heavy nuclei has greatly attracted researchers attention which theoretical mechanism of cluster decay is regarded as quantum mechanical tunneling through the potential barrier between cluster emitter and the residual daughter nucleus. At this study, calculation of potential barrier is critical part. At present, many theoretical approaches have been used to describe the cluster-decay, such as the macroscopic-microscopic model[3], Density-dependent cluster model[4–6] relativistic mean field theory [7, 8]. in these models, various nuclear potential is used for calculation of half-lives and spectroscopic properties. The liquid drop model, double-folding model and proximity are example of most potential that are applied recently [9–16]. One of the successful and applicable models is by using the proximity potential which is a function of separation between the surfaces of the two nuclei. Many versions of proximity potential are proposed by different groups in order to improve the model [17–22]. Interestingly, the temperature dependence of proximity model has been modified by some authors to study fusion reactions and barrier characteristic[22].

At previous work, we studied the influence of the temperature of the parent nucleus on the alpha-decay process by applying the temperature dependence of the proximity potential and transfer matrix approach to calculate the penetration probability[23]. In this work, we attempt to study the cluster-decay half-lives of parent nuclei by considering the temperature dependence of the proximity potential and using WKB approach for calculating the penetration probability across the potential barrier. The structure of this paper is as follows: In sec. II, modified proximity model with temperature dependence is briefly introduced. In sec. III, half-lives of emitted ^{14}C , $^{18,20}\text{O}$, ^{23}F , $^{22,24,25,26}\text{Ne}$, $^{28,30}\text{Mg}$ and ^{34}Si cluster are compared with existing experimental values. In addition, half-lives of heavy nuclei are calculated theoretically and compared with analytical relation based on the ASAF model [2]. Finally the conclusion is given in Sec. IV.

II. MODEL

In the cluster model the parent nucleus is assumed to be the interaction between the cluster particle and daughter nucleus where the total potential is equal to the sum of the nuclear potential, the coulomb potential and centrifugal barrier. Thus,

$$V(R) = V_N(R) + V_C(R) + \hbar^2 l(l+1)/(2\mu R^2) \quad (1)$$

Where μ is the reduced mass and $V_C(R)$, the Coulomb interaction potential is given by,

$$V_C(R) = \begin{cases} Z_e Z_d e^2 / R & \text{for } R \geq R_c \\ (Z_e Z_d e^2 / 2R)(3 - (R/R_c)^2) & \text{for } R \leq R_c \end{cases} \quad (2)$$

in above equation, R_c is expressed by, $R_c = 1.24(R_e + R_d)$, R_e and R_d are respectively the radii of emitted cluster and daughter nuclei. However, Z_e and Z_d represents the charge number of emitted cluster and daughter nuclei respectively.

Using the proximity theorem we can obtain a simple formula for nuclear potential between emitted clusters and residual daughter nuclei as a function of the separation distance between the surfaces of them [17].

$$V_N(r) = 4\pi\gamma b \bar{R} \Phi(\xi) \quad \text{MeV}. \quad (3)$$

Here \bar{R} is the reduced radius and is written as:

$$\bar{R} = \frac{C_1 C_2}{C_1 + C_2} \quad (4)$$

and

$$C_i = R_i \left[1 - \left(\frac{b}{R_i} \right)^2 + \dots \right]. \quad (5)$$

where b is the surface width and R_i is the effective sharp radius, and given by:

$$R_i = 1.28 A_i^{1/3} - 0.76 + 0.8 A_i^{-1/3} \text{ fm} \quad (i = 1, 2). \quad (6)$$

In Eq. (1), $\Phi(\xi)$ is the universal function which has been derived by several authors in different forms [20, 21] and in original proximity version was defined as:

$$\Phi(\xi) \begin{cases} -\frac{1}{2}(\xi - 2.54)^2 - 0.0852(\xi - 2.54)^3 & \xi \leq 1.2511 \\ -3.437 e^{-\xi/0.75} & \xi > 1.2511 \end{cases} \quad (7)$$

and the surface energy coefficient defines as a function of the neutron/proton excess as:

$$\gamma = \gamma_0[1 - k_s A_s^2] \quad (8)$$

where $A_s = (\frac{N-Z}{N+Z})$ and γ_0 and K_s are the surface energy and surface asymmetry constants respectively. These constants have different values in different proximity potential versions and they revised to $K_s = 4$ and $\gamma_0 = 1.460734 \text{ Mev}/\text{fm}^2$ for to the proximity-2010 [21] that we used in this work . In order to achieve an exact form of proximity potential where be able to reproduce the experimental data more accurately, many researches have been done which led to different versions for proximity potentials [24–26]. In one of these attempts, proximity-2010 is modified with a temperature dependence of surface energy coefficient and it has been successful in expecting the fusion barrier data and the experimental fusion cross section [22].

$$\gamma(T) = \gamma(T = 0)[1 - \frac{T - T_B}{T_B}]^{3/2} \quad (9)$$

where T_B is the temperature associated with the energies near the Coulomb barrier.

Temperature dependency, also followed in some other parts of the proximity potential as:

$$R_i(T) = R_i(T = 0)[1 + 0.0005T^2] \text{fm} (i = 1, 2) \quad (10)$$

and,

$$b(T) = b(T = 0)[1 + 0.009T^2] \quad (11)$$

The temperature T in Eqs. (9-11) can be expressed as [27, 28],

$$E_{CN}^* = E_{c.m.} + Q_{in} = \frac{1}{9}AT^2 - T. \quad (12)$$

Here, E_{CN}^* denotes the excitation energy of parent nucleus with mass number A . Q_{in} denote the entrance channel Q-value of the system and $E_{c.m.}$ is the center-of-mass incident energy which according to Refs. [22, 29] , one can use the following definition

$$E_{c.m.} = \frac{e^2 Z_e Z_d}{R_1 + R_2 + 2} \quad (13)$$

where the radius $R_{1,2}$ is obtained by Eq. (6). In order to explore the temperature effects of parents nucleus in this study, we have employed all three above relations simultaneously in proximity-2010 potential, and we have calculated the interaction potential in this way. With the shape of total cluster-nucleus potential, one can calculate the penetration probability

as well as half-life $T_{1/2}$ of the parent nucleus. According to the WKB approximation the penetration probability is calculated by,

$$P = \exp \left[-\frac{2}{\hbar} \int_{R_{\text{in}}}^{R_{\text{out}}} \sqrt{2\mu(R)[V(R) - Q]} dR \right] \quad (14)$$

Where $\mu(R)$ is the effective mass of the cluster particle and the daughter nucleus which is set as the reduced mass. Q is released energy for which experimental values are used in the present calculations. R_{in} and R_{out} denote the classical turning points inside and outside of the barrier which are determined from the equation $V(R_{\text{in}}) = V(R_{\text{out}}) = Q$.

The cluster-decay half-life $T_{1/2}$ is then calculated with the penetration probability [30],

$$T_{1/2} = \frac{h \ln 2}{2E_\nu P}. \quad (15)$$

Where E_ν denotes the zero point the empirical vibration energy is given by [31],

$$E_\nu = Q[0.056 + 0.039e^{\frac{4-A_e}{2.5}}] \quad (16)$$

where A_e is the mass number of emitted cluster nuclei

III. RESULTS

In this section at first we test our calculation for the existing measured values of half-lives. after investigate the role of temperature dependence on cluster decay half-lives, then we will apply this formalism for calculation of cluster decay half-lives.

III-A. compare to experimental data

In order to test the precision of our calculation, we compare the calculated results with the existing experimental data[32] of the half-lives. We gets the 28 parents nuclei which cluster decays includes ^{14}C , $^{18,20}\text{O}$, ^{23}F , $^{22,24,25,26}\text{Ne}$, $^{28,30}\text{Mg}$ and ^{34}Si . It is relevant to mention here that the selected cluster nuclei were discovered from the experiments[33, 34]. In Table-I, we compared measured experimental data and the calculated half-lives of cluster decay with including the temperature effect of parent nucleus(TD.) and without the temperature effect(IND.). also the minimum angular momentum l_{min} carried away by the emitted cluster is determined by the principle of spin-parity conservation when the nuclei are decayed and

the values are from [35]. In order to give some indication of the quality of the results, the last line of table-I also shows the relative error,

$$\chi_R^2 = \frac{1}{N} \sum_{i=1}^N \left[\frac{Y^{Exp.} - Y^{Th.}}{Y^{Exp.} + Y^{Th.}} \right]^2, \quad (17)$$

where $Y = \log_{10} T_{1/2}$. This quantity shows the deviation of the calculated half-lives from the experimental values. It is clear that corresponding values of χ_R^2 for temperature dependent is less than ignoring the temperature effects one.

In order to show better the ability of our method on calculations of cluster decay half-lives, we define hindrance factor as follow:

$$HF = \frac{T_{1/2}^{Exp.}}{T_{1/2}^{Cal}} \quad (18)$$

Figure-1 depicts the comparison of HF between temperature dependence of proximity potential (TD.) and temperature independent (IND.). as the definition of HF clear that closer to unity is more accurate results we have. This figure reveals that TD. results are motivating. therefore it seems we can apply this method for calculation of cluster decay for heavy nuclei.

III-B. Calculation of cluster decay for heavy nuclei

In Table-II we list the theoretical cluster decay half-lives of temperature dependent proximity potential and prediction of ASAF model [2] ones for nuclei with Z parent between 56 and 120. The first column of Table-II denotes nuclide. The experimental Q cluster-decay energy (Q_c) is given in column 2. When the Q_c is not known, we use a theoretical value from ref. [36]. The logarithmic cluster decay half-lives with TD. and ASAF model [2] ones are listed in columns 3 and 4, respectively. The last column is the reference the error between calculation of our work and ASAF model. It is seen from Table-II that TD. half-lives are reasonable estimates.

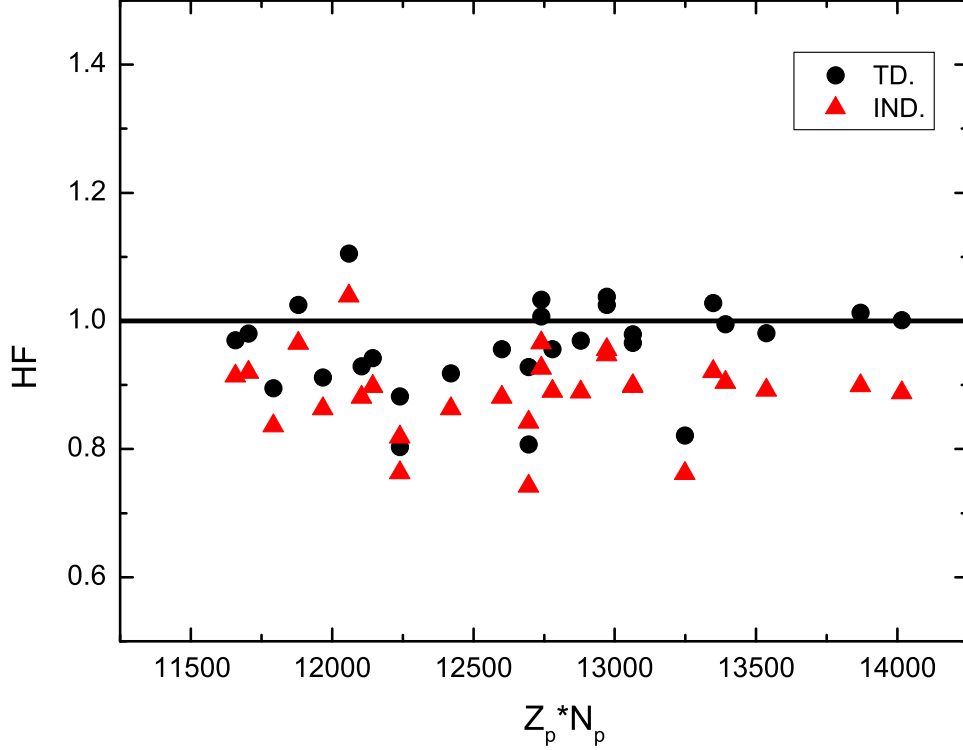


FIG. 1: Comparison between hindrance factor of temperature dependence of cluster decays half-lives (TD.) and independent case (IND.).

IV. CONCLUSION

By using the temperature dependent proximity potential, we calculated cluster decay half-lives of parent nuclei whose proton numbers are from $Z_p = 56$ to $Z_p = 120$. Before the calculation, we test the accuracy of the our calculation for some nuclei in compare with experimental data. The results of present calculation made with T.D. model are in good agreement with experimental data (see Table-I and Figure-1). at next, T.D. model calculation are provided in Table-II for cluster decay half-lives of heavy nuclei and compared with the values based on the ASAF model [2] estimation using the same $Q - values$. this formalism has been found to be quit reliable.

ACKNOWLEDGMENTS

The authors would like to give special thanks to Dr. F. Zanganeh for helpful discussions

and encouragements.

- [1] S. Kumar, Phys. Rev. C 85, 024320 (2012).
- [2] D. N. Poenaru and et al. Phys. Rev. C 65, 054308 (2002).
- [3] M. Mirea, A. Sandulescu and D. S. Delion, Nucl. Phys. A 870, 23 (2011).
- [4] D. Ni and Z. Ren, Phys. Rev. C 83, 014310 (2011).
- [5] D. Ni and Z. Ren, Phys. Rev. C 81, 024315 (2010).
- [6] F. R. Xu and J. C. Pei, nucl-th/0603064 (2006).
- [7] M. Bhuyan, S. K. Patra and R. K. Gupta, Phys. Rev. C 84, 014317 (2011).
- [8] P. Roy. Choudhury, G. Gangopadhyay and A. Bhattacharyya, Phys. Rev. C 83, 027601 (2011).
- [9] B. Buck, A. C. Merchant and S. M. Perez, Phys. Rev. C 45, 2247 (1992).
- [10] B. Buck, A. C. Merchant and S. M. Perez, Data Nucl. Data Tables 54, 53 (1993).
- [11] C. Xu and Z. Ren, Phys. Rev. C 69, 024614 (2004).
- [12] P. Mohr Phys. Rev. C 61, 045802 (2000).
- [13] U. Atzrott, P. Mohr, H. Abele, C. Hillenmayer and G. Staudt, Phys. Rev. C 53, 1336 (1996).
- [14] C. Xu and Z. Ren, Nucl. Phys. A 760, 303 (2005).
- [15] Z. Ren, C. Xu and Z. Wang, Phys. Rev. C 70, 034304 (2004).
- [16] P. R. Chowdhury, C. Samanta and D. N. Basu, Phys. Rev. C 73, 014612 (2006).
- [17] J. Blocki, J. Randrup, W. J. Swiatecki, and C.F.Tsang, Ann. Phys. (NY) 105, 427 (1977).
- [18] G. Royer and J. Mignen, J. Phys. G: Nucl. Part. Phys. 18, 1781 (1992).
- [19] S. Shlomo and J. B. Natowitz, Phys. Rev. C 44, 2878 (1991).
- [20] W. D. Myers, Phys. Rev. C 62, 17 (2000).
- [21] I. Dutt and R. K. Puri, Phys. Rev. C 81, 047601 (2010).
- [22] M.Salehi and O. N. Ghodsi, Chin. Phys. Lett. 30, No.4, 042502 (2013).
- [23] V. Zanganeh and N. Wang, Nucl. Phys. A 929, 94 (2014).
- [24] A. Winther, Nucl. Phys. A 594,203 (1995).
- [25] H. Ngo and C. Ngo, Nucl. Phys. A 348, 140 (1980).
- [26] V. Y. Denisov, Phys. Lett. B 526, 315 (2002).
- [27] R. K. Puri and R. K. Gupta, J. Phys. G: Nucl. Part. Phys. 18, 903 (1992).
- [28] R. K. Gupta, S. Singh, R. K. Puri, A. Sandulescu,W. Greiner andW. Scheid, J. Phys. G: Nucl.

- Part. Phys. 18, 1533 (1992).
- [29] M. Golshanian, O. N. Ghodsi, and R. Gharæi, *Mod. Phys. Lett. A*, vol. 28, no. 36, pp. 113, (2013).
- [30] S. A. Gurvitz, G. Kalbermann, *Phys. Rev. Lett.* 59, 262 (1987).
- [31] D.N. Poenaru, M. Ivascu, A. Sandulescu, W. Greiner, *Phys. Rev. C* 32, 572 (1985).
- [32] G. Royer, R. Moustabchir, *Nucl. Phys. A* 683, 182 (2001).
- [33] H. J. Rose, G. A. Jones, *Nature* 307, 245 (1984).
- [34] D. V. Aleksandrov, et al., *JETP. Lett.* 40, 909 (1984).
- [35] D. N. Basu, *Phys. Lett. B* 566, 90 (2003).
- [36] G. Audi and et al. , *Chin. Phys. C* 36, 1157 (2012).

TABLE CAPTIONS

Table-I: Comparison of logarithmic half-lives of cluster decays between temperature independent proximity ($IND.$), temperature dependent proximity ($TD.$) and experiment data

cluster decay	lmin	$Q_{exp.}$	$IND.$	$TD.$	$Exp.$	$\Delta^{IND.}$	$\Delta^{TD.}$
$^{221}\text{Fr} \rightarrow ^{14}\text{C}$	3	31.29	15.86	14.94	14.5	-1.36	-0.44
$^{221}\text{Ra} \rightarrow ^{14}\text{C}$	3	32.40	14.56	13.66	13.4	-1.16	-0.26
$^{222}\text{Ra} \rightarrow ^{14}\text{C}$	0	33.05	13.15	12.28	11.0	-2.15	-1.28
$^{223}\text{Ra} \rightarrow ^{14}\text{C}$	4	31.83	15.75	14.82	15.2	-0.55	0.37
$^{224}\text{Ra} \rightarrow ^{14}\text{C}$	0	30.54	18.19	17.22	15.7	-2.49	-1.52
$^{226}\text{Ra} \rightarrow ^{14}\text{C}$	0	28.19	23.61	22.51	21.2	-2.41	-1.31
$^{225}\text{Ac} \rightarrow ^{14}\text{C}$	4	30.47	19.52	18.52	17.2	-2.32	-1.32
$^{226}\text{Th} \rightarrow ^{14}\text{C}$	0	30.55	20.04	19.04	15.3	-4.74	-3.74
$^{226}\text{Th} \rightarrow ^{18}\text{O}$	0	45.73	20.50	19.05	16.8	-3.70	-2.25
$^{224}\text{Th} \rightarrow ^{14}\text{C}$	0	32.93	15.11	14.20	15.7	0.58	1.49
$^{228}\text{Th} \rightarrow ^{20}\text{O}$	0	44.73	23.97	22.53	20.7	-3.27	-1.83
$^{231}\text{Pa} \rightarrow ^{23}\text{F}$	1	51.85	26.90	25.16	26.0	-0.90	0.83
$^{230}\text{U} \rightarrow ^{22}\text{Ne}$	0	61.39	23.27	21.11	19.6	-3.67	-1.51
$^{230}\text{Th} \rightarrow ^{24}\text{Ne}$	0	57.76	27.92	25.72	24.6	-3.32	-1.12
$^{231}\text{Pa} \rightarrow ^{24}\text{Ne}$	1	60.41	24.71	22.73	22.9	-1.81	0.16
$^{230}\text{U} \rightarrow ^{24}\text{Ne}$	0	61.35	24.51	22.56	18.2	-6.31	-4.36
$^{232}\text{U} \rightarrow ^{24}\text{Ne}$	0	62.31	22.94	21.05	20.4	-2.54	-0.65
$^{233}\text{U} \rightarrow ^{24}\text{Ne}$	2	60.49	25.97	23.89	24.8	-1.17	0.90
$^{234}\text{U} \rightarrow ^{24}\text{Ne}$	0	58.83	28.91	26.55	26.0	-2.91	-0.55
$^{233}\text{U} \rightarrow ^{25}\text{Ne}$	2	60.73	26.17	24.19	24.8	-1.37	0.60
$^{232}\text{Th} \rightarrow ^{26}\text{Ne}$	0	55.97	32.56	30.32	29.0	-3.56	-1.32
$^{234}\text{U} \rightarrow ^{26}\text{Ne}$	0	59.47	28.94	26.91	26.0	-2.94	-0.91
$^{236}\text{U} \rightarrow ^{26}\text{Ne}$	0	56.75	34.10	31.67	26.0	-8.10	-5.67

cluster decay	lmin	$Q_{exp.}$	$IND.$	$TD.$	$Exp.$	$\Delta^{IND.}$	$\Delta^{TD.}$
$^{236}\text{Pu} \rightarrow ^{28}\text{Mg}$	0	79.67	23.55	21.10	21.7	-1.85	0.59
$^{237}\text{Np} \rightarrow ^{30}\text{Mg}$	2	74.79	30.53	27.74	27.6	-2.93	-0.14
$^{238}\text{Pu} \rightarrow ^{30}\text{Mg}$	0	76.80	28.81	26.19	25.7	-3.11	-0.49
$^{241}\text{Am} \rightarrow ^{34}\text{Si}$	3	93.93	28.13	24.97	25.3	-2.83	0.32
$^{242}\text{Cm} \rightarrow ^{34}\text{Si}$	0	96.52	26.13	23.17	23.2	-2.93	0.02
$\chi_R^2 * 10^{-3}$	—	—	4.96	1.91	—	—	—

Table-II: Comparison of the calculated logarithmic half-lives between temperature dependent proximity (TD.) with results based on ASAF model [2].

cluster decay	ASAF	TD.	Δ	cluster decay	ASAF	TD.	Δ
$^{114}\text{Ba} \rightarrow ^{12}\text{C}$	10.760	10.714	-0.046	$^{232}\text{Pa} \rightarrow ^{23}\text{F}$	27.041	28.081	1.040
$^{117}\text{Ba} \rightarrow ^{12}\text{C}$	21.159	21.623	0.464	$^{232}\text{U} \rightarrow ^{26}\text{Ne}$	28.735	29.535	0.800
$^{119}\text{Ba} \rightarrow ^{12}\text{C}$	24.044	24.624	0.580	$^{232}\text{Pu} \rightarrow ^{22}\text{Ne}$	21.116	22.124	1.008
$^{120}\text{La} \rightarrow ^{12}\text{C}$	23.668	24.256	0.587	$^{233}\text{U} \rightarrow ^{25}\text{Ne}$	23.707	24.162	0.455
$^{121}\text{La} \rightarrow ^{12}\text{C}$	27.208	27.940	0.732	$^{233}\text{U} \rightarrow ^{28}\text{Mg}$	25.106	25.918	0.813
$^{122}\text{Ce} \rightarrow ^{12}\text{C}$	26.027	26.741	0.714	$^{233}\text{Np} \rightarrow ^{24}\text{Ne}$	22.049	22.519	0.470
$^{124}\text{Ce} \rightarrow ^{12}\text{C}$	34.286	35.304	1.018	$^{233}\text{Pu} \rightarrow ^{22}\text{Ne}$	23.483	24.967	1.484
$^{215}\text{At} \rightarrow ^8\text{Be}$	15.358	16.694	1.336	$^{234}\text{U} \rightarrow ^{24}\text{Ne}$	25.367	26.550	1.183
$^{218}\text{Ra} \rightarrow ^{12}\text{C}$	14.007	15.194	1.186	$^{234}\text{U} \rightarrow ^{28}\text{Mg}$	25.176	26.074	0.898
$^{222}\text{Ac} \rightarrow ^{12}\text{C}$	12.934	14.093	1.159	$^{234}\text{Np} \rightarrow ^{28}\text{Mg}$	22.795	23.059	0.264
$^{223}\text{Th} \rightarrow ^{15}\text{N}$	16.878	17.940	1.062	$^{234}\text{Pu} \rightarrow ^{28}\text{Mg}$	21.889	21.856	-0.033
$^{225}\text{Np} \rightarrow ^{12}\text{C}$	9.911	10.645	0.734	$^{235}\text{U} \rightarrow ^{25}\text{Ne}$	27.945	29.198	1.254
$^{225}\text{U} \rightarrow ^{15}\text{N}$	16.845	17.857	1.012	$^{235}\text{U} \rightarrow ^{28}\text{Mg}$	27.560	29.050	1.490
$^{227}\text{Th} \rightarrow ^{22}\text{Ne}$	25.220	27.049	1.829	$^{235}\text{Np} \rightarrow ^{28}\text{Mg}$	22.879	23.228	0.349
$^{228}\text{Pu} \rightarrow ^{15}\text{N}$	18.105	19.258	1.152	$^{235}\text{Pu} \rightarrow ^{25}\text{Ne}$	26.781	27.633	0.852
$^{228}\text{Th} \rightarrow ^{24}\text{Ne}$	25.307	26.338	1.031	$^{235}\text{Pu} \rightarrow ^{29}\text{Mg}$	25.538	25.911	0.373
$^{228}\text{Pa} \rightarrow ^{22}\text{Ne}$	22.038	23.266	1.228	$^{236}\text{U} \rightarrow ^{26}\text{Ne}$	30.376	31.677	1.301
$^{229}\text{Ac} \rightarrow ^{22}\text{O}$	26.916	27.595	0.679	$^{114}\text{Ba} \rightarrow ^{16}\text{O}$	15.192	14.988	-0.204
$^{229}\text{Th} \rightarrow ^{24}\text{Ne}$	24.642	25.623	0.981	$^{117}\text{Ba} \rightarrow ^{16}\text{O}$	24.113	24.468	0.355
$^{229}\text{Pa} \rightarrow ^{23}\text{F}$	27.024	27.898	0.875	$^{119}\text{Ba} \rightarrow ^{16}\text{O}$	27.517	28.064	0.548
$^{229}\text{Pa} \rightarrow ^{24}\text{Ne}$	23.278	23.935	0.656	$^{120}\text{Ce} \rightarrow ^{16}\text{O}$	17.415	17.388	-0.027
$^{230}\text{Th} \rightarrow ^{23}\text{F}$	28.734	29.995	1.261	$^{121}\text{Ce} \rightarrow ^{16}\text{O}$	19.671	19.799	0.129
$^{230}\text{Pa} \rightarrow ^{23}\text{F}$	25.436	26.150	0.714	$^{123}\text{Ce} \rightarrow ^{16}\text{O}$	24.949	25.413	0.464
$^{230}\text{Pa} \rightarrow ^{22}\text{Ne}$	25.066	26.958	1.892	$^{124}\text{Pr} \rightarrow ^{16}\text{O}$	24.196	24.645	0.449
$^{230}\text{U} \rightarrow ^{24}\text{Ne}$	22.139	22.566	0.428	$^{218}\text{Fr} \rightarrow ^8\text{Be}$	10.856	11.924	1.067
$^{231}\text{U} \rightarrow ^{22}\text{Ne}$	22.688	24.111	1.423	$^{221}\text{Pa} \rightarrow ^8\text{Be}$	8.441	9.279	0.838

cluster decay	ASAF	TD.	Δ	cluster decay	ASAF	TD.	Δ
$^{231}\text{Th} \rightarrow ^{25}\text{Ne}$	26.970	28.056	1.086	$^{222}\text{Ac} \rightarrow ^{15}\text{N}$	14.665	15.497	0.832
$^{231}\text{Pa} \rightarrow ^{23}\text{F}$	24.509	25.152	0.643	$^{223}\text{Th} \rightarrow ^{17}\text{O}$	19.915	21.289	1.374
$^{231}\text{Np} \rightarrow ^{22}\text{Ne}$	20.605	21.555	0.950	$^{225}\text{Pa} \rightarrow ^{15}\text{N}$	14.445	15.235	0.789
$^{227}\text{U} \rightarrow ^{17}\text{O}$	18.959	20.233	1.274	$^{235}\text{U} \rightarrow ^{29}\text{Mg}$	27.959	29.076	1.117
$^{227}\text{Pa} \rightarrow ^{22}\text{Ne}$	22.813	24.119	1.306	$^{235}\text{Np} \rightarrow ^{29}\text{Mg}$	27.498	28.386	0.887
$^{228}\text{Th} \rightarrow ^{22}\text{Ne}$	25.723	27.714	1.991	$^{235}\text{Pu} \rightarrow ^{28}\text{Mg}$	21.263	21.151	-0.112
$^{228}\text{Ac} \rightarrow ^{23}\text{F}$	28.811	30.074	1.263	$^{236}\text{U} \rightarrow ^{24}\text{Ne}$	29.604	31.640	2.036
$^{228}\text{U} \rightarrow ^{22}\text{Ne}$	20.768	21.681	0.912	$^{236}\text{U} \rightarrow ^{30}\text{Mg}$	29.083	30.084	1.001
$^{229}\text{Ac} \rightarrow ^{23}\text{F}$	27.984	29.195	1.211	$^{236}\text{Np} \rightarrow ^{28}\text{Mg}$	25.100	25.992	0.891
$^{229}\text{U} \rightarrow ^{22}\text{Ne}$	19.874	20.682	0.809	$^{236}\text{Np} \rightarrow ^{30}\text{Mg}$	27.581	28.140	0.559
$^{229}\text{Pa} \rightarrow ^{22}\text{Ne}$	22.306	23.642	1.336	$^{236}\text{Pu} \rightarrow ^{29}\text{Mg}$	26.214	26.785	0.572
$^{230}\text{Th} \rightarrow ^{22}\text{O}$	26.388	26.962	0.575	$^{237}\text{Np} \rightarrow ^{30}\text{Mg}$	27.163	27.708	0.545
$^{230}\text{Th} \rightarrow ^{24}\text{Ne}$	24.674	25.724	1.050	$^{237}\text{Pu} \rightarrow ^{29}\text{Mg}$	24.362	24.614	0.252
$^{230}\text{Pa} \rightarrow ^{24}\text{Ne}$	22.249	22.793	0.544	$^{237}\text{Pu} \rightarrow ^{32}\text{Si}$	25.273	25.624	0.351
$^{230}\text{U} \rightarrow ^{20}\text{O}$	25.653	26.672	1.019	$^{237}\text{Am} \rightarrow ^{29}\text{Mg}$	27.384	28.142	0.758
$^{231}\text{Pa} \rightarrow ^{22}\text{O}$	29.269	30.111	0.842	$^{238}\text{Pu} \rightarrow ^{28}\text{Mg}$	25.341	26.288	0.947
$^{231}\text{Th} \rightarrow ^{24}\text{Ne}$	27.253	28.795	1.542	$^{238}\text{Pu} \rightarrow ^{30}\text{Mg}$	25.954	26.195	0.240
$^{231}\text{U} \rightarrow ^{22}\text{O}$	33.553	34.746	1.193	$^{238}\text{Pu} \rightarrow ^{33}\text{Si}$	28.717	29.571	0.854
$^{231}\text{Pa} \rightarrow ^{24}\text{Ne}$	22.144	22.722	0.579	$^{238}\text{Am} \rightarrow ^{29}\text{Mg}$	25.778	26.267	0.490
$^{232}\text{Th} \rightarrow ^{26}\text{Ne}$	29.211	30.325	1.114	$^{238}\text{Am} \rightarrow ^{32}\text{Si}$	23.191	22.941	-0.250
$^{232}\text{U} \rightarrow ^{24}\text{Ne}$	20.755	21.050	0.295	$^{238}\text{Cm} \rightarrow ^{28}\text{Mg}$	22.733	22.893	0.159
$^{232}\text{U} \rightarrow ^{28}\text{Mg}$	25.065	25.804	0.739	$^{239}\text{Pu} \rightarrow ^{30}\text{Mg}$	27.997	28.712	0.715
$^{233}\text{U} \rightarrow ^{24}\text{Ne}$	23.106	23.847	0.741	$^{239}\text{Pu} \rightarrow ^{34}\text{Si}$	27.318	27.455	0.137
$^{233}\text{U} \rightarrow ^{26}\text{Ne}$	27.197	27.825	0.628	$^{239}\text{Am} \rightarrow ^{32}\text{Si}$	23.367	23.227	-0.140
$^{233}\text{Np} \rightarrow ^{22}\text{Ne}$	26.062	28.111	2.049	$^{239}\text{Am} \rightarrow ^{34}\text{Si}$	26.224	25.957	-0.267
$^{233}\text{Np} \rightarrow ^{25}\text{Ne}$	27.596	28.557	0.961	$^{240}\text{Pu} \rightarrow ^{34}\text{Si}$	27.029	27.170	0.141
$^{233}\text{Pu} \rightarrow ^{24}\text{Ne}$	22.945	23.473	0.527	$^{240}\text{Am} \rightarrow ^{34}\text{Si}$	25.576	25.215	-0.361
$^{234}\text{U} \rightarrow ^{26}\text{Ne}$	26.359	26.914	0.555	$^{240}\text{Cm} \rightarrow ^{32}\text{Si}$	21.634	20.979	-0.655
$^{234}\text{Np} \rightarrow ^{25}\text{Ne}$	25.498	26.186	0.688	$^{241}\text{Am} \rightarrow ^{33}\text{Si}$	28.547	29.451	0.904
$^{234}\text{Pu} \rightarrow ^{24}\text{Ne}$	23.037	23.629	0.592	$^{241}\text{Cm} \rightarrow ^{32}\text{Si}$	23.649	23.592	-0.058

cluster decay	ASAF	TD.	Δ	cluster decay	ASAF	TD.	Δ
$^{235}\text{U} \rightarrow ^{24}\text{Ne}$	27.478	29.079	1.601	$^{242}\text{Cm} \rightarrow ^{34}\text{Si}$	23.938	23.174	-0.764
$^{235}\text{U} \rightarrow ^{26}\text{Ne}$	28.323	29.244	0.921	$^{242}\text{Cf} \rightarrow ^{33}\text{Si}$	26.205	26.179	-0.026
$^{242}\text{Cf} \rightarrow ^{36}\text{S}$	24.037	23.064	-0.973	$^{237}\text{Am} \rightarrow ^{28}\text{Mg}$	22.160	22.243	0.083
$^{244}\text{Cm} \rightarrow ^{34}\text{Si}$	27.261	27.461	0.200	$^{237}\text{Am} \rightarrow ^{32}\text{Si}$	23.567	23.352	-0.215
$^{244}\text{Cf} \rightarrow ^{36}\text{S}$	23.781	22.852	-0.929	$^{238}\text{Pu} \rightarrow ^{29}\text{Mg}$	28.028	29.105	1.077
$^{249}\text{Cf} \rightarrow ^{42}\text{S}$	31.708	30.886	-0.822	$^{238}\text{Pu} \rightarrow ^{32}\text{Si}$	25.484	25.966	0.482
$^{249}\text{No} \rightarrow ^{48}\text{Ca}$	27.237	23.322	-3.915	$^{238}\text{Am} \rightarrow ^{28}\text{Mg}$	23.892	24.410	0.518
$^{250}\text{No} \rightarrow ^{48}\text{Ca}$	26.894	22.916	-3.979	$^{238}\text{Am} \rightarrow ^{30}\text{Mg}$	28.052	28.592	0.540
$^{251}\text{No} \rightarrow ^{48}\text{Ca}$	26.646	22.633	-4.013	$^{238}\text{Am} \rightarrow ^{33}\text{Si}$	26.006	26.035	0.029
$^{252}\text{Cf} \rightarrow ^{50}\text{Ca}$	32.209	30.055	-2.154	$^{238}\text{Cm} \rightarrow ^{32}\text{Si}$	22.065	21.411	-0.655
$^{252}\text{No} \rightarrow ^{48}\text{Ca}$	26.321	22.250	-4.071	$^{239}\text{Pu} \rightarrow ^{33}\text{Si}$	27.436	28.043	0.608
$^{253}\text{No} \rightarrow ^{48}\text{Ca}$	26.069	21.964	-4.105	$^{239}\text{Am} \rightarrow ^{30}\text{Mg}$	27.533	28.027	0.494
$^{253}\text{Fm} \rightarrow ^{48}\text{Ca}$	27.932	24.796	-3.137	$^{239}\text{Am} \rightarrow ^{33}\text{Si}$	26.563	26.798	0.236
$^{254}\text{No} \rightarrow ^{46}\text{Ca}$	26.810	23.880	-2.930	$^{239}\text{Cm} \rightarrow ^{32}\text{Si}$	21.546	20.818	-0.728
$^{254}\text{No} \rightarrow ^{50}\text{Ca}$	29.401	25.731	-3.670	$^{240}\text{Am} \rightarrow ^{33}\text{Si}$	25.545	25.602	0.056
$^{255}\text{No} \rightarrow ^{50}\text{Ca}$	28.718	24.871	-3.846	$^{240}\text{Cm} \rightarrow ^{30}\text{Mg}$	28.773	29.466	0.693
$^{256}\text{No} \rightarrow ^{50}\text{Ca}$	27.896	23.813	-4.083	$^{240}\text{Cm} \rightarrow ^{34}\text{Si}$	25.142	24.544	-0.598
$^{257}\text{No} \rightarrow ^{50}\text{Ca}$	27.034	22.714	-4.320	$^{241}\text{Am} \rightarrow ^{34}\text{Si}$	25.285	24.923	-0.362
$^{258}\text{No} \rightarrow ^{48}\text{Ca}$	27.071	23.640	-3.431	$^{242}\text{Cm} \rightarrow ^{32}\text{Si}$	25.389	25.858	0.469
$^{258}\text{Rf} \rightarrow ^{48}\text{Ca}$	25.519	21.218	-4.301	$^{242}\text{Cf} \rightarrow ^{32}\text{Si}$	22.321	21.737	-0.584
$^{258}\text{Rf} \rightarrow ^{50}\text{Ca}$	28.953	25.076	-3.876	$^{242}\text{Cf} \rightarrow ^{34}\text{Si}$	26.373	25.969	-0.404
$^{258}\text{Rf} \rightarrow ^{51}\text{Ti}$	27.699	23.286	-4.413	$^{243}\text{Cm} \rightarrow ^{34}\text{Si}$	25.638	25.360	-0.278
$^{258}\text{Rf} \rightarrow ^{53}\text{Ti}$	29.963	25.593	-4.370	$^{244}\text{Cf} \rightarrow ^{34}\text{Si}$	25.575	25.095	-0.480
$^{259}\text{No} \rightarrow ^{48}\text{Ca}$	28.184	25.229	-2.955	$^{246}\text{Cf} \rightarrow ^{38}\text{S}$	26.050	25.058	-0.991
$^{260}\text{No} \rightarrow ^{48}\text{Ca}$	29.194	26.700	-2.493	$^{249}\text{Cf} \rightarrow ^{46}\text{Ar}$	31.476	29.809	-1.668
$^{261}\text{No} \rightarrow ^{50}\text{Ca}$	29.409	26.204	-3.205	$^{249}\text{Cf} \rightarrow ^{50}\text{Ca}$	33.768	31.906	-1.862
$^{236}\text{Np} \rightarrow ^{29}\text{Mg}$	26.044	26.701	0.657	$^{251}\text{Cf} \rightarrow ^{46}\text{Ar}$	30.023	28.044	-1.979
$^{236}\text{Pu} \rightarrow ^{28}\text{Mg}$	21.180	21.107	-0.073	$^{252}\text{Cf} \rightarrow ^{46}\text{Ar}$	29.450	27.371	-2.079
$^{236}\text{Pu} \rightarrow ^{30}\text{Mg}$	27.608	28.051	0.444	$^{252}\text{Md} \rightarrow ^{46}\text{Ca}$	28.135	25.713	-2.422

cluster decay	ASAF	TD.	Δ	cluster decay	ASAF	TD.	Δ
$^{237}\text{Np} \rightarrow ^{32}\text{Si}$	27.691	28.824	1.133	$^{290}\text{Lv} \rightarrow ^{28}\text{Mg}$	28.151	31.051	2.900
$^{237}\text{Pu} \rightarrow ^{30}\text{Mg}$	26.473	26.752	0.279	$^{294}118 \rightarrow ^{50}\text{Ca}$	30.932	28.049	-2.883
$^{254}\text{Md} \rightarrow ^{48}\text{Ca}$	26.229	22.387	-3.843	$^{252}\text{No} \rightarrow ^{50}\text{Ca}$	30.370	26.912	-3.458
$^{254}\text{No} \rightarrow ^{48}\text{Ca}$	25.771	21.616	-4.155	$^{253}\text{No} \rightarrow ^{50}\text{Ca}$	29.953	26.411	-3.542
$^{255}\text{No} \rightarrow ^{48}\text{Ca}$	25.129	20.802	-4.328	$^{294}118 \rightarrow ^{48}\text{Ca}$	28.298	25.294	-3.004
$^{256}\text{No} \rightarrow ^{48}\text{Ca}$	24.856	20.481	-4.374	$^{294}118 \rightarrow ^{34}\text{Si}$	28.340	29.541	1.202
$^{257}\text{No} \rightarrow ^{48}\text{Ca}$	25.982	22.075	-3.907	$^{294}118 \rightarrow ^{28}\text{Mg}$	26.362	28.647	2.285
$^{258}\text{Md} \rightarrow ^{50}\text{Ca}$	28.580	25.039	-3.540	$^{296}120 \rightarrow ^{50}\text{Ca}$	29.703	26.144	-3.559
$^{258}\text{No} \rightarrow ^{50}\text{Ca}$	26.552	22.117	-4.435	$^{296}120 \rightarrow ^{48}\text{Ca}$	26.588	22.688	-3.900
$^{258}\text{Rf} \rightarrow ^{49}\text{Ca}$	27.898	24.045	-3.854	$^{296}120 \rightarrow ^{34}\text{Si}$	26.225	26.588	0.362
$^{258}\text{Rf} \rightarrow ^{50}\text{Ti}$	26.451	21.964	-4.488	$^{296}120 \rightarrow ^{28}\text{Mg}$	23.811	25.164	1.353
$^{258}\text{Rf} \rightarrow ^{52}\text{Ti}$	27.570	22.681	-4.889	$^{296}120 \rightarrow ^{22}\text{Ne}$	21.380	23.695	2.315
$^{258}\text{Rf} \rightarrow ^{54}\text{Ti}$	30.359	25.722	-4.636				
$^{259}\text{No} \rightarrow ^{50}\text{Ca}$	27.544	23.526	-4.019				
$^{261}\text{No} \rightarrow ^{48}\text{Ca}$	30.204	28.182	-2.022				
$^{262}\text{No} \rightarrow ^{50}\text{Ca}$	30.314	27.526	-2.788				
$^{271}\text{Sg} \rightarrow ^{50}\text{Ca}$	35.508	34.739	-0.769				
$^{271}\text{Sg} \rightarrow ^{48}\text{Ca}$	35.301	35.561	0.260				
$^{275}\text{Hs} \rightarrow ^{50}\text{Ca}$	34.793	33.712	-1.081				
$^{275}\text{Hs} \rightarrow ^{48}\text{Ca}$	33.969	33.627	-0.342				
$^{275}\text{Hs} \rightarrow ^{34}\text{Si}$	32.585	35.222	2.637				
$^{272}\text{Ds} \rightarrow ^{50}\text{Ca}$	32.760	30.290	-2.471				
$^{272}\text{Ds} \rightarrow ^{48}\text{Ca}$	30.114	27.558	-2.556				
$^{272}\text{Ds} \rightarrow ^{34}\text{Si}$	29.647	30.659	1.012				
$^{272}\text{Ds} \rightarrow ^{28}\text{Mg}$	26.760	28.470	1.710				
$^{272}\text{Ds} \rightarrow ^{22}\text{Ne}$	26.238	29.287	3.049				
$^{290}\text{Lv} \rightarrow ^{50}\text{Ca}$	32.079	29.703	-2.375				
$^{290}\text{Lv} \rightarrow ^{48}\text{Ca}$	29.710	27.344	-2.367				
$^{290}\text{Lv} \rightarrow ^{34}\text{Si}$	29.450	31.000	1.550				